Geo-Mar Lett (2015) 35:271–288
DOI 10.1007/s00367-015-0406-6

ORIGINAL

# Erosional and depositional contourite features at the transition between the western Scotia Sea and southern South Atlantic Ocean: links with regional water-mass circulation since the Middle Miocene

**Lara F. Pérez[1,7] · F. Javier Hernández-Molina[2] · Federico D. Esteban[3] · Alejandro Tassone[3] · Alberto R. Piola[4] · Andrés Maldonado[1] · Benedict Preu[5] · Roberto A. Violante[4] · Emanuele Lodolo[6]**

Received: 8 November 2014 / Accepted: 27 March 2015 / Published online: 9 May 2015


**Abstract** The aim of the present study was to characterise the morpho-sedimentary features and main stratigraphic stacking pattern off the Tierra del Fuego continental margin, the north-western sector of the Scotia Sea abyssal plain (Yaghan Basin) and the Malvinas/Falkland depression, based on single- and multi-channel seismic profiles. Distinct contourite features were identified within the sedimentary record from the Middle Miocene onwards. Each major drift developed in a water depth range coincident with a particular water mass, contourite terraces on top of some of these drifts being associated with interfaces between water masses. Two major palaeoceanographic changes were identified. One took place in the Middle Miocene with the onset of Antarctic Intermediate Water flow and the enhancement of Circumpolar Deep Water (CDW) flow, coevally with the onset of Weddell Sea Deep Water flow in the Scotia Sea. Another palaeoceanographic change occurred on the abyssal plain of the Yaghan Basin in the Late Miocene as a consequence of the onset of Southeast Pacific Deep Water flow and its complex interaction with the lower branch of the CDW. Interestingly, these two periods of change in bottom currents are coincident with regional tectonic episodes, as well as climate and Antarctic ice sheet oscillations. The results convincingly demonstrate that the identification of contourite features on the present-day seafloor and within the sedimentary record is the key for decoding the circulation of water masses in the past. Nevertheless, further detailed studies, especially the recovery of drill cores, are necessary to establish a more robust chronology of the evolutionary stages at the transition between the western Scotia Sea and the southern South Atlantic Ocean.

✉ Lara F. Pérez
larafperez@gmail.com

[1] Instituto Andaluz de Ciencias de la Tierra, Avda. de las Palmeras 4, 18100 Armilla, Granada, Spain

[2] Department of Earth Sciences, Royal Holloway University of London, Egham, Surrey TW20 0EX, UK

[3] Instituto de Geociencias Básicas, Ambientales, Aplicadas, Departamento de Ciencias Geológicas, University of Buenos Aires, Buenos Aires, Argentina

[4] Servicio de Hidrografía Naval, Montes de Oca 2124, Buenos Aires C1270ABV, Argentina

[5] Chevron Upstream Europe, Chevron North Sea Ltd, Seafield House, Aberdeen AB15 6XL, UK

[6] Istituto Nazionale di Oceanografia e di Geofisica Sperimentale, 34010 Sgonico, Trieste, Italy

[7] Present address: Geophysical Department, Geological Survey of Denmark and Greenland, Øester Voldgade 10, 1350 Copenhagen K, Denmark

## Introduction

Marine bottom currents play a key role in the formation of specific depositional, erosional and mixed features such as contourite drifts and terraces. These features have been identified in various settings worldwide, together with their associations with major palaeoceanographic events (for recent overview, see Rebesco et al. 2014). Between South America and the Antarctic Peninsula, the Drake Passage is a critical area for global climatic changes, as its opening enabled the development of a circumpolar circulation (Kennett 1977; Lawver and Gahagan 2003; Maldonado et al. 2014). To the east of the Drake Passage, the Scotia Sea is influenced by the water masses flowing through this gateway (e.g. Orsi et al.

1999). Due to its relatively shallow bathymetry (Fig. 1), the northern boundary of the Scotia Sea—the North Scotia Ridge (NSR)—represents a major morphologic obstacle to the northward flow of Scotia Sea water masses (Howe et al. 1997; Smith et al. 2010). Nevertheless, some water-mass exchange between the Scotia Sea and the South Atlantic Ocean (Howe et al. 1997; Hernández-Molina et al. 2010) would influence the supply and distribution of sediments along both sides of the NSR which, as a consequence, should contain unique records of any palaeoceanographic changes.

Indeed, bottom current influence has been documented in the sedimentary record of the southern sector of the Scotia Sea (Maldonado et al. 2003, 2006; Pérez et al. 2014) where it reflects the onset of the Weddell Sea Deep Water circulation and its interaction with the Circumpolar Deep Water. In the case of the NSR, the action of bottom water masses is related to the palaeo-current regime of the circumpolar circulation (Lodolo et al. 2006). Very recently, Owen et al. (2014) reported an influence of the Antarctic Circumpolar Current in the northeast of the Scotia Sea. In the Malvinas/Falkland Trough, current-related features are associated with the existence of an internal recirculation loop (Howe et al. 1997; Cunningham et al. 1998; Koenitz et al. 2008). Along the western edge of the NSR, along-slope sedimentary processes have not been explored yet, and potential effects of bottom current action are unknown to date. Based on regional oceanographic knowledge, bottom currents in this area should have a significant influence on the present-day seafloor morphology as well as the sedimentary evolution of the continental margins.

Within this context, the aim of the present study was to identify major regional contourite features across the transition between the western Scotia Sea and the southern South Atlantic Ocean, to explore their relationships with present-day circulation and how this has affected the evolution of the continental margins in the geologic past. The investigation is based on seismo-stratigraphic and morpho-sedimentary analyses, as well as a syn-sedimentary tectonic analysis integrated into a water-mass evolutionary model spanning the Middle Miocene to present times.

## Geological setting

The study area is located in the north-western sector of the Scotia Sea, off the Tierra del Fuego margin and Isla de los Estados (also known as Staten Island; Fig. 1). This is a structurally complex region resulting from the superimposition of different tectonic phases during the Late Cretaceous and the Palaeogene (Klepeis and Austin 1997; Lawver and Gahagan 2003; Eagles and Jokat 2014). The North Scotia Ridge (NSR), which is roughly E–W oriented, comprises fragments of continental crust such as the Burdwood, Davis and Aurora (or Barker) banks, the emerged Shag and Black rocks, and South Georgia Island (e.g. Ludwig et al. 1968; Davey 1972). The NSR incorporates part of the offshore sector of the Magallanes-Fagnano fault system, a major segment of the South America–Scotia plate boundary (Lodolo et al. 2003, 2006), and represents the continuation of the emerged orogenic system of the southern Patagonian Andes (Platt and Philip 1995; Bry et al. 2004).

The southern flank of the NSR represents a combined sheared passive margin which structurally continues westwards to the Beagle Channel fault system (Fig. 1c; Lodolo et al. 2003). The northern flank of the NSR involves the fold and thrust belt formed during the Andean orogeny, and is the front of an accretionary prism created by active subduction of the South America plate beneath the Scotia plate (Ludwig et al. 1968; Cunningham 1993; Klepeis and Austin 1997; Tassone et al. 2008). This active convergence has given rise to the northern Malvinas/Falkland Trough (Ewing et al. 1971), an E–W bathymetric depression located between 56°W and 41°W (Fig. 1). To the west of the trough, the subduction developed a bathymetric depression (Cunningham and Barker 1996), hereafter referred to as the Malvinas/Falkland depression. In addition, active thrusting has been reported to occur at the foot of the Burdwood Bank (Ludwig and Rabinowitz 1982; Platt and Philip 1995; Richards et al. 1996; Bry et al. 2004).

## Oceanographic setting

Located between the southern tip of South America and the Antarctic Peninsula, the Drake Passage and the adjacent Scotia Sea represent one of the most important oceanic gateways on Earth, where water masses are being exchanged between the Pacific and Atlantic oceans as well as the Weddell Sea (e.g. Barker and Thomas 2004; Eagles and Jokat 2014). Below the surface water masses, the Antarctic Intermediate Water (AAIW) is formed by mixing and northward downwelling along the Antarctic Convergence/Antarctic Polar Front with minor modifications by sea–air interaction within the Scotia Sea (Naveira Garabato et al. 2003). Underneath the AAIW, the Circumpolar Deep Water (CDW) constitutes the deepest part of the Antarctic Circumpolar Current (ACC) and flows eastwards through the Scotia Sea (Orsi et al. 1999). The CDW comprises an upper (UCDW) and lower (LCDW) part.

The Southeast Pacific Deep Slope Water (SPDSW) flows along the southern continental slope of South America and reaches the Scotia Sea via the northern Drake Passage (Well et al. 2003), circulating between the UCDW and the LCDW (Fig. 2). The abyssal plain between the Southern Antarctic Circumpolar Current Front and the Polar Front is occupied by the Southeast Pacific Deep Water (SPDW), which flows eastwards from the south-eastern Pacific Ocean through the Drake Passage (Sievers and Nowlin 1984; Arhan et al. 1999; Naveira Garabato et al. 2002a). Within the northwest Scotia

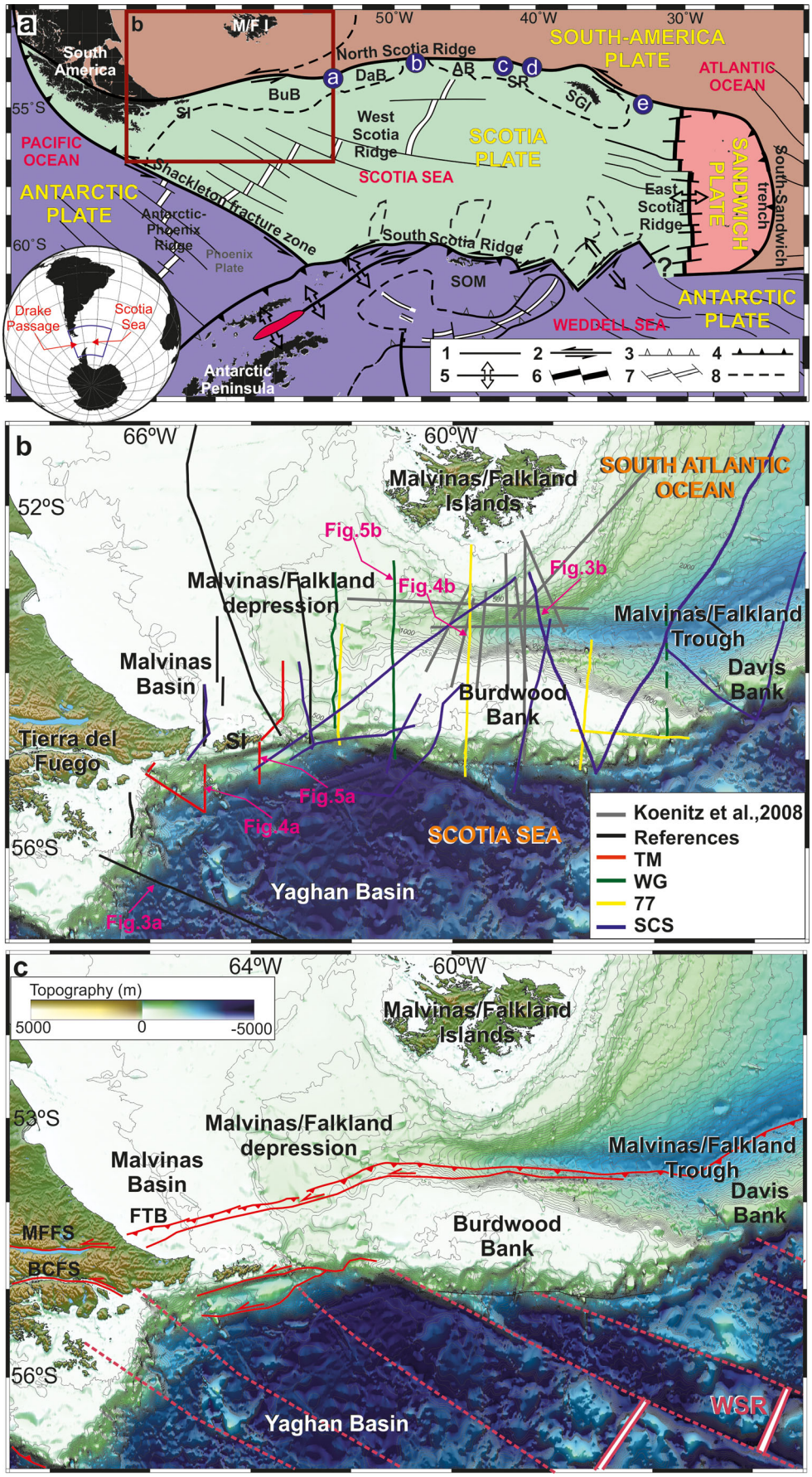


**Fig. 1** **a** Tectonic setting of the Scotia Sea (modified from Maldonado et al. 2000; Galindo-Zaldivar et al. 2006). *1* Transform fault, *2* active transcurrent fault, *3* inactive subduction zone, *4* active subduction zone, *5* active extensional zone, *6* active spreading centre, *7* inactive spreading centre, *8* continental–oceanic crust boundary, *AB* Aurora Bank, *BuB* Burdwood Bank, *DaB* Davis Bank, *SGI* South Georgia Island, *SI* Staten Island (Isla de los Estados), *SOM* South Orkney microcontinent, *SR* Shag and Black rocks. NSR passages for water-mass outflow (*blue circles*): *a* 54-54, *b* Davis-Aurora, *c* Shag Rocks, *d* Black Rocks, *e* South Georgia. **b** Simplified bathymetric map of the western sector of the NSR (extracted from Sandwell and Smith 1997), with locations of seismic profiles used in the present study. **c** Main structural features offshore Tierra del Fuego. *Dotted red lines* Fracture zones of West Scotia Ridge (WSR). *BCFS* Beagle Channel fault system, *FTB* fault and thrust belt, *MFFS* Magallanes-Fagnano fault system

Sea, enhancement of the SPDW and CDW promotes the development of strong clockwise and counter-clockwise deep-water eddies (Fig. 2; Tarakanov 2009, 2012; Morozov et al. 2010). To the south of the Southern Antarctic Circumpolar Current Front, the Scotia Sea abyssal plain is occupied by the Weddell Sea Deep Water (WSDW), which derives from the Weddell Gyre and flows both eastwards and westwards (Orsi et al. 1999).

Along the crest of the NSR the water depth ranges from 200 to 2,000 m, except at the Shag Rocks Passage (Fig. 1a) which forms an approx. 3,100-m-deep gap in the ridge (Deacon 1933; Zenk 1981). As a consequence, the NSR constrains the vertical structure of the ACC by forming a barrier to northward flow of its deep components (Fig. 2). Shallower water masses, such as the Antarctic Surface Water and the AAIW, cross the NSR and then flow to the northeast to form the Malvinas/Falkland Current (Fig. 2; Peterson and Whitworth 1989; Piola and Gordon 1989; Muñoz et al. 2012). At greater depths, a small amount of CDW is transported northwards over the shallower part of the NSR east of 45°W (Naveira Garabato et al. 2002a). The UCDW exits the Scotia Sea between the Isla de los Estados margin and the Burdwood Bank, and the 54-54 Passage (Smith et al. 2010). In contrast, the bulk of the LCDW flows northwards through the Shag Rocks Passage (Naveira Garabato et al. 2002a), a minor portion also crossing the Black Rocks Passage (Figs. 1a, 2; Smith et al. 2010).

The pathways of the SPDW leaving the Scotia Sea remain a subject of debate. Generally speaking, most of the SPDW presumably flows through the Scotia Sea up to the Georgia Passage (Fig. 1a; Meredith et al. 2001; Naveira Garabato et al. 2002a). There is also some controversy about whether the WSDW is primarily transported across the NSR (Locarnini et al. 1993; Cunningham et al. 1998; Arhan et al. 1999; Smith et al. 2010). Most lines of evidence suggest that the WSDW flows into the South Atlantic Ocean through the South Sandwich Trench and the Georgia Passage (Fig. 1a; Georgi 1981; Naveira Garabato et al. 2002b; Smith et al. 2010). Outside the Scotia and Weddell seas this water mass is usually referred to as Antarctic Bottom Water (AABW; e.g. Wittstock and Zenk 1983; Locarnini et al. 1993; Orsi et al. 1999).

North of the NSR, these waters masses describe a relatively sharp clockwise loop. They flow westwards along the southern flank of the Malvinas/Falkland Trough, returning eastwards along its northern flank (Figs. 1a, 2; Cunningham and Barker 1996; Howe et al. 1997; Cunningham et al. 1998; Hernández-Molina et al. 2009, 2010).

## Materials, methods, data sources

Regional morpho-sedimentary and seismo-stratigraphic assessments were carried out on the basis of single- and multi-channel seismic surveys (SCS and MCS respectively) conducted along the western end of the NSR (Fig. 1b). The seismic data sources comprise (1) published profiles used as reference data (see Ludwig and Rabinowitz 1982; Cunningham et al. 1998; Lodolo et al. 2006; Tassone et al. 2008; Anderson et al. 2010); (2) publicly available SCS profiles from the National Geophysical Data Center/NOAA and Marine Geoscience Data System/ASP-UTIG; (3) industrial seismic

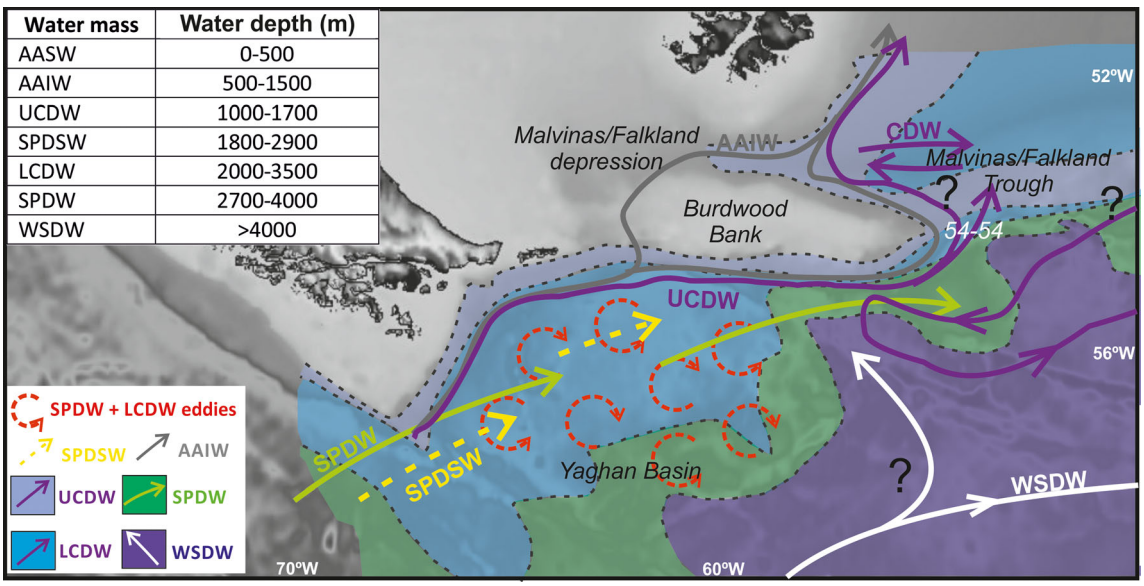


**Fig. 2** Distribution of main water masses along the western Scotia–Atlantic edge. *Dotted lines* Interfaces (based on Tarakanov 2009, 2012; Morozov et al. 2010). Water-mass depth ranges based on Ingle (2000), Naveira Garabato et al. (2002a, 2003), Well et al. (2003), Smith et al. (2010). *AASW* Antarctic Surface Water, *AAIW* Antarctic Intermediate Water, *CDW* Circumpolar Deep Water, *LCDW* Lower CDW, *SPDSW* Southeast Pacific Deep Slope Water, *SPDW* Southeast Pacific Deep Water, *UCDW* Upper CDW, *WSDW* Weddell Sea Deep Water

profiles provided by the Daniel Valencio Geophysical Institute and Secretaría de Minería Argentina (WG, 77 data); (4) MCS data acquired during a 1999 geophysical cruise of the TESAC project (TM data), and partially published by Lodolo et al. (2006). The reader is referred to that publication and Geletti et al. (2005) for details on the seismic acquisition systems and data processing, as well as the website of the UTIG.

The seismic data were interpreted using the commercially available software package Kingdom Suite™. Isobath and isopach maps were generated by means of simple gridding interpolation between the seismic profiles aided by bathymetric information. The seismo-stratigraphic analyses were laterally correlated with the results of Galeazzi (1998), Koenitz et al. (2008) and Baristeas et al. (2013) from the northern NSR basins, and stratigraphic data from the Scotia Sea (Geletti et al. 2005; Maldonado et al. 2006). To extend the characterisation and spatial distribution of plastered drifts and contourite terraces, in particular the findings of Koenitz et al. (2008) from the Malvinas/Falkland Trough were used, including their Fig. 4a (with permission from John Wiley & Sons). Depth and thickness in the stratigraphic column are expressed in seconds two-way travel time (TWTT). Where necessary, a water-column wave velocity of 1,500 m/s was chosen for depth conversion.

World Ocean Database 2009 (WOD09) was used as a source for hydrographic data to create the joint hydrographic and seismic cross-sections. Due to the lack of synoptic hydrographic sections, the cross-slope sections were prepared by combining all available CTD datasets, the water sample stations being projected onto the seismic cross-section. To reduce the noise imparted by the variability of water masses along the profiles, the fields were smoothed to represent time-mean property distributions. This approach provided a sufficiently large data pool to suppress smaller local features and seasonal events. Hydrographic profiles were created using Ocean Data View (Schlitzer 2013).

### Names and terminology

The northwest Scotia Sea abyssal plain adjacent to the Tierra del Fuego continental margin is commonly called the Yaghan Basin (Fig. 1b; cf. Provost et al. 2011). This nomenclature is retained in the present study for the margins and abyssal plain of the northwest Scotia Sea.

An unconformity at the base of the sedimentary record is here referred to as the (*acoustic*) *basement top*. Stratigraphic discontinuities bounding seismic units are *stratigraphic horizons* or just *horizons*.

The term *contourite* refers to sediments deposited or substantially reworked by the persistent action of bottom currents (e.g. Stow et al. 2002; Rebesco 2005; Rebesco et al. 2014). Thick, extensive sedimentary accumulations are called *contourite drifts* or *drifts*. The present work adopts the classification of Faugères et al. (1999), later modified by Faugères and Stow (2008). Low-gradient, along-slope, slightly seaward-dipping surfaces produced by erosional and depositional processes related to water-mass circulation are here defined as *contourite terraces*. In the wider study region and elsewhere, these are commonly related to deep pycnoclines characterised by strong spatiotemporal variations (e.g. Viana 2001; Hernández-Molina et al. 2009, 2014; Preu et al. 2013; Rebesco et al. 2014). Finally, a set of similar depositional and erosional contourite features is defined in terms of an equivalent position within the slope sedimentary sequence, specific names being attributed to each feature (e.g. drift $P_b$), although these could be laterally discontinuous.

## Results

### Main present-day erosional and depositional features

A set of depositional and erosional contourite features has been identified along the Yaghan Basin (Fig. 3a). Over the upper slope, a plastered drift ($P_a$) is commonly located between 350 and 700 m water depth (wd). Deeper on the upper slope, another plastered drift ($P_b$) occurs between 800 and 1,500 m wd (Fig. 3). To the east of the basin, the latter depth range incorporates an infill drift sandwiched between the basement highs. An elongated and mounded drift ($M_a$) has been identified on the western middle slope between 1,600 and 2,700 m wd, which is currently being eroded (Fig. 4a). A very well-developed sheeted drift ($Sh_a$) is found in the western part at the base of the slope between 3,500 and 4,000 m wd. A set of mounded drifts ($M_b$) occurs in the abyssal plain at a water depth of about 3,750 m where the drifts are usually confined by structural highs (Fig. 3).

Major erosional and mixed features comprise abraded surfaces and contourite terraces. The main abraded surfaces are located in the west between 850 and 2,600 m wd (Fig. 4a), dipping to the east. Of the two major terraces (Figs. 3, 4a), $T_a$, lies between 900 and 1,100 m wd and dips to the northeast, its width progressively reducing from ca. 10 km to 2 km. $T_b$ is situated on the western middle slope on top of the $M_a$ drift between 1,700 and 2,000 m wd. It is strongly incised by three roughly N–S-oriented canyons (Fig. 4a).

Within the Malvinas/Falkland depression, the seafloor is strongly conditioned by the morphology of the Malvinas/Falkland Trough. Its depth increases to the east where a plastered drift ($P_b$) has been identified between 700 and 1,100 m wd, attached to the south-western slope of the Malvinas/Falkland Islands. A sheeted drift ($Sh_b$) adjacent to the sharp northern boundary of the Burdwood Bank is located at about 1,100 m wd (Fig. 4b). Regarding the erosional and mixed morphologic elements, the main abraded surfaces are located around the edges of Burdwood Bank, at depths of 600 to 1,300 m

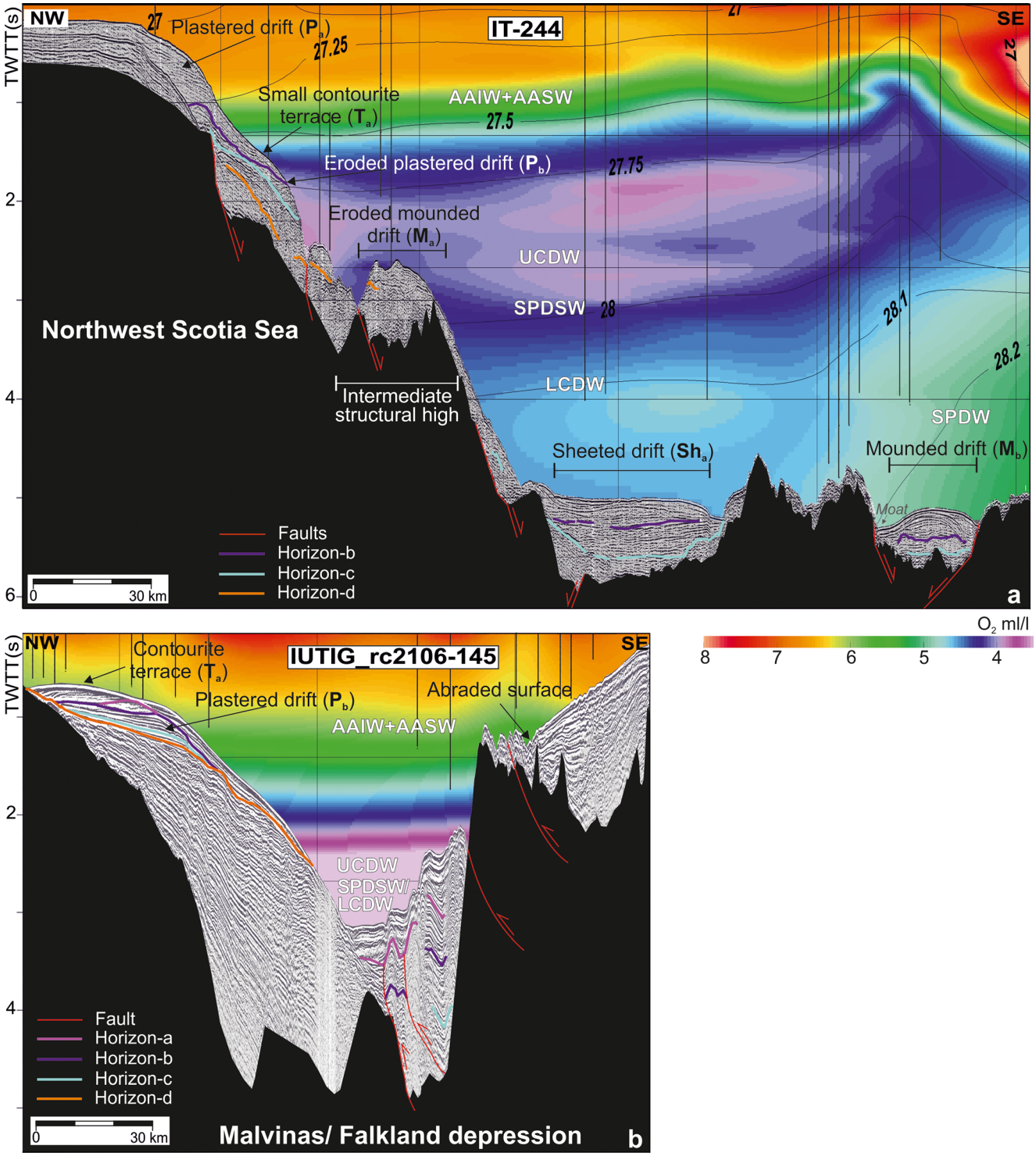


**Fig. 3** Seismic and hydrographic vertical sections of **a** the Yaghan Basin and **b** the Malvinas/Falkland depression (see Fig. 1b for profile locations). Note that $T_a$ and $P_a$ are not completely visible; they extend to the northeast, as can be seen in the bathymetry in Fig. 1b. *Solid lines* CTD-station locations

(Fig. 4b). The terrace-shaped feature $T_a$ is also present in this area at 400–600 m wd on the south-western slope of the Malvinas/Falkland Islands. This terrace is about 6 km wide but exceeds 10 km farther east, slightly dipping into the trench (according to data from Koenitz et al. 2008).

## Main regional structural elements

The top of the acoustic basement is clearly identifiable as a high-amplitude reflection throughout the study area (Figs. 4, 5). The basement depth of the Yaghan Basin ranges from 1 s

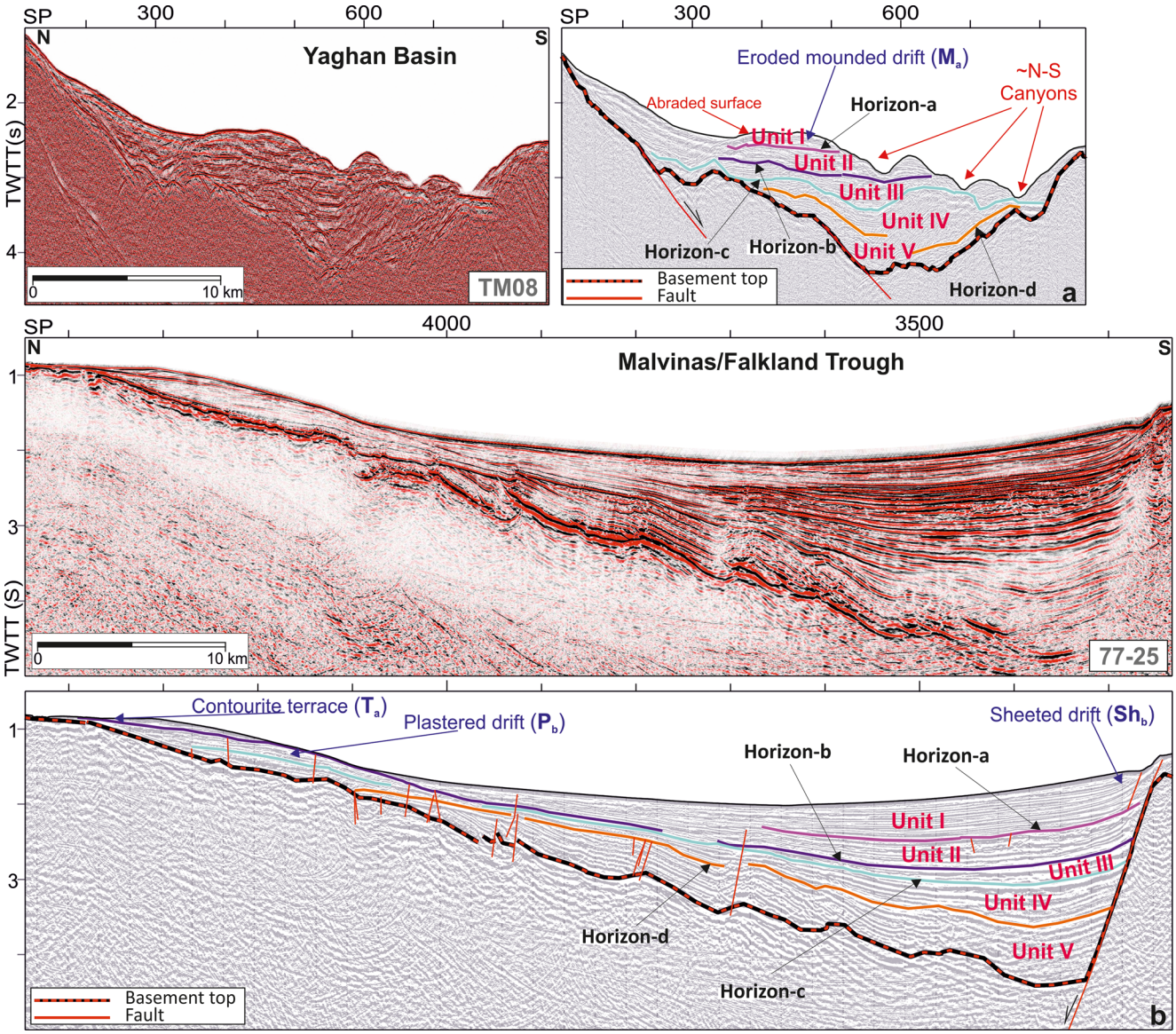


**Fig. 4** Regional seismic cross-sections of **a** the Yaghan Basin margin (*left* profile TM08 MCS, *right* interpretation) and **b** east of the Malvinas/Falkland depression (*top* profile 77-25 MCS, *bottom* interpretation). See Fig. 1b for profile locations

TWTT on the upper slope to 6 s TWTT in the abyssal plain (Fig. 6a). In the Malvinas/Falkland depression, the trend of the acoustic basement top follows the eastward deepening of the seafloor (>7 s TWTT).

The Yaghan Basin is characterised by a highly fractured margin (Fig. 5a). The acoustic basement is disrupted by sub-vertical faults which also affect the lowermost sedimentary record. Normal faults widely cutting the crust reflections are common along the zone of major morphological changes. From north to south, the rough topography dips to the abyssal plain through a sub-vertical escarpment comprising a normal fault trace. On the western side, this bathymetric drop is slightly smoothed by an intermediate structural high (~25 km wide) which leads to a strongly deformed depression (~14 km wide). Internally, this high is formed by asymmetric and tilted blocks cut by sub-vertical, southward-dipping faults (Fig. 4a). Regarding the structural characteristics of the Malvinas/Falkland depression, the northern flank of the Burdwood Bank is characterised by NW thrust faults, whereas the southern flank of the Malvinas/Falkland Islands is characterised by sub-vertical normal faults which affect both the igneous crust and the lower part of the sedimentary record (Fig. 5b).

## Seismic stratigraphy

The sedimentary record is characterised by highly variable thickness (Fig. 6b). The Yaghan Basin has a reduced average thickness (~0.5 s TWTT) compared to the Malvinas/Falkland depression (~2 s TWTT), where mean sediment thickness increases towards the trough (eastwards) and exceeds 3 s

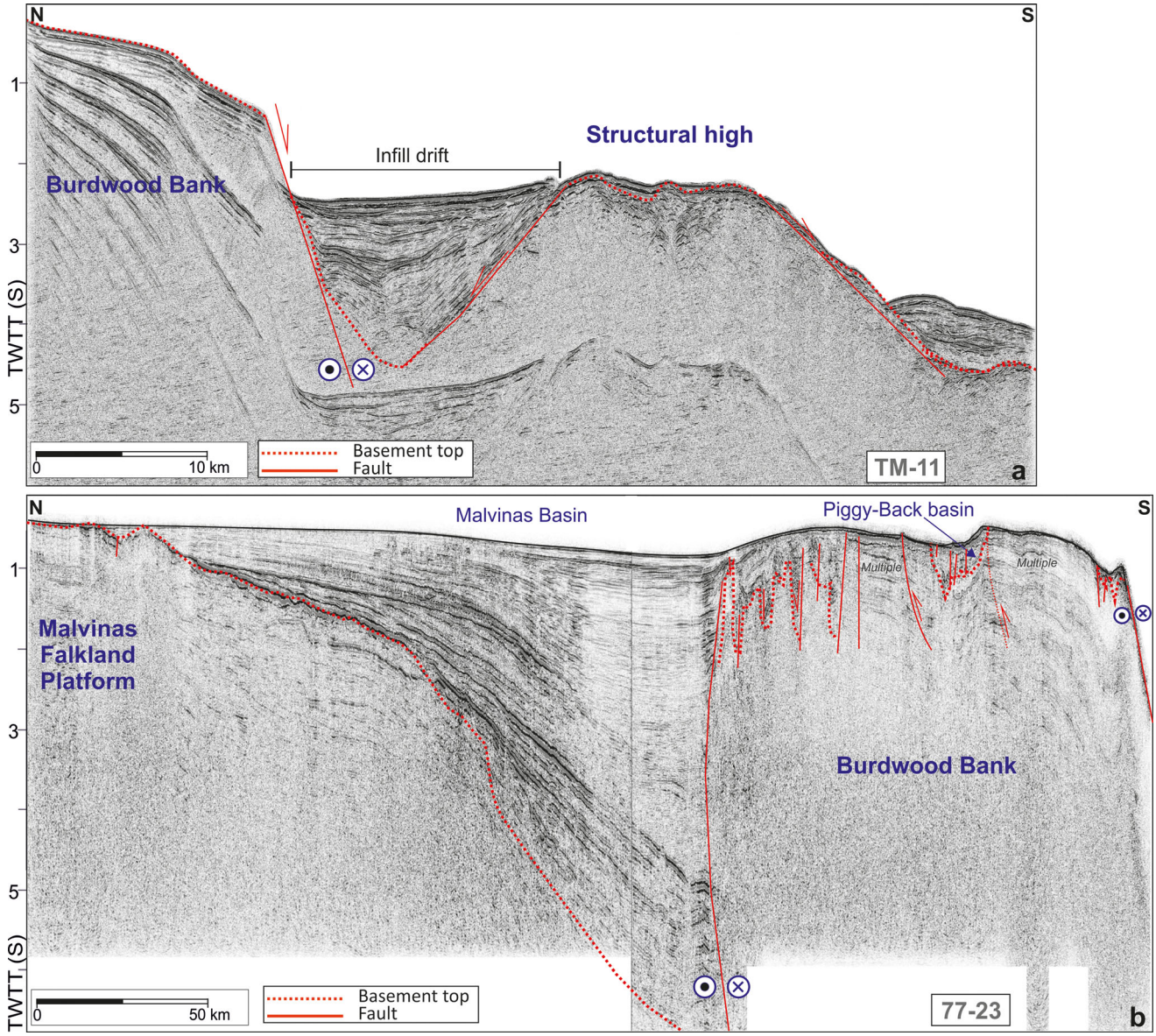


**Fig. 5** Regional seismic cross-sections of **a** the Yaghan Basin margin (profile TM11) and **b** the Malvinas/Falkland depression (profile 77-23). See Fig. 1b for profile locations

TWTT. On the Yaghan Basin slope, two depocentres with thicknesses >1 s TWTT have been identified (Fig. 6b), matching with deeper basement depressions which are infilled with sediments (Fig. 5a).

Five seismic units can be distinguished within the sedimentary record, from bottom to top referred to as *units V* to *I*. Their boundaries are formed by high-amplitude, laterally continuous reflections which locally represent stratigraphic unconformities. In upward stratigraphic order, these reflections are referred to as *horizons d* to *a* (Fig. 4). The discontinuities are generally deeper in the Yaghan Basin abyssal plain than in the Malvinas/Falkland depression, where all discontinuities tilt towards the trough, just as the internal reflections of the units do. A brief description of the seismic facies of each unit and the stratigraphic signature of each discontinuity is provided in Table 1. Horizon c is the most prominent reflection, being a high-amplitude reflection and generally the most strongly eroded surface (Figs. 3, 4). Moreover, the units below horizon c (units V and IV; hereafter, the *lower units*) exhibit different seismic facies than do the units above it (units III, II and I; hereafter, the *upper units*). Also horizon b represents a prominent discontinuity, particularly in the Yaghan Basin where this high-amplitude reflection terminates the underlying toplapping reflections.

In the Yaghan Basin the lower units are characterized by low amplitudes. They reach their maximum thickness (>0.5 s TWTT) along the western edge, parallel to the foot of the slope and coinciding with the greatest basement depths (Figs. 4a, 7a). In the Malvinas/Falkland depression, the lower units are formed by high-amplitude reflections and their

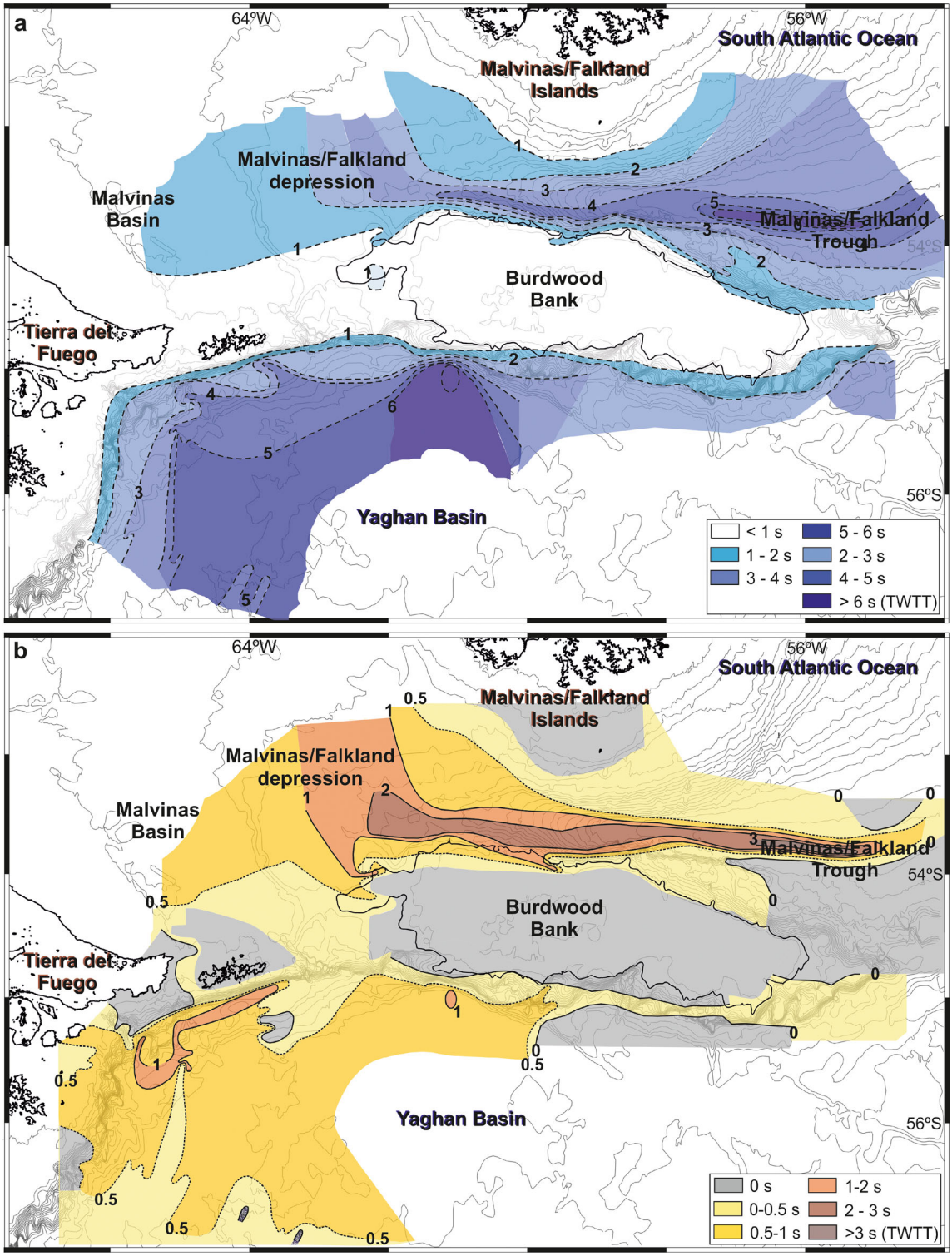


**Fig. 6** **a** Depth contours of acoustic basement top and **b** thickness distribution of sedimentary record in the study area (both datasets in s TWTT)

wedge morphology fills the trough. The thickness increases to the southeast, and the main depocentre (>1 s TWTT) follows the trend of the trough, sharply thinning along the northern margin of Burdwood Bank (Figs. 4b, 6a, 7a).

In the Yaghan Basin the amplitudes of the internal reflections of the upper units are higher than those of the lower units. The upper units present drift morphologies which are particularly well developed in the western part (Figs. 3a, 4a). To the east, the main drifts ($Sh_a$ and $M_b$) are restricted to units

**Table 1** Main stratigraphic characteristics of units and horizons

| | Malvinas/Falkland Depression | Yaghan Basin |
|---|---|---|
| Unit I | Few reflections of high amplitude, high lateral continuity, thickness 0.3–0.5 s (TWTT) | Few reflections of high amplitude, high lateral continuity, thickness 0.3–0.5 s (TWTT) |
| *Horizon a* | Middle amplitude, maximum depth 1.2–2.2 s, W–E | Middle amplitude, maximum depth 2.6–3.5 s, W–E |
| Unit II | High amplitude, middle lateral continuity, thickness 0.3–0.5 s, E–W | High amplitude, middle lateral continuity, thickness 0.2–0.3 s |
| *Horizon b* | Low amplitude, maximum depth 2.9 s | High amplitude, depth 3.9–4.1 s |
| Unit III | Low amplitude, evenly continuous, maximum thickness ~0.8 s | High amplitude, high continuity, average thickness ~0.4 s |
| *Horizon c* | Depth tilts 1.2–2.9 s | N depth range 3.5–4.8 s, S depth range 1.6–5.6 s |
| Unit IV | Few reflections of high amplitude, high lateral continuity, chaotic in the N, tilt to the trench, maximum thickness ~0.7 s | Middle amplitude, middle lateral continuity (discontinuous zones), widespread extension, average thickness ~0.5 s |
| *Horizon d* | Strong high-amplitude tilt, depth 2.2–3.6 s | Weak, average depth 4.5 s |
| Unit V | High amplitude, high lateral continuity, highly deformed and tilted to S, maximum thickness 0.8 s | Low amplitude, low lateral continuity decreasing downwards, maximum thickness 1 s |

II and I, whereas along the slope the three upper units form mounded and plastered drifts. In their distribution the upper units follow the morphology of the slope, but their depocentres (>0.5 s TWTT) are located north of those of the lower units (Fig. 7). The reflections of the upper units in the Malvinas/Falkland depression have lower amplitudes and exhibit wavy or drift morphologies superimposed on their wedge shape. The main contouritic features ($Sh_b$; Fig. 4b) are restricted to unit I, whereas $P_b$ comprises the three upper units. Nonetheless, in the central and eastern sectors, all three upper units comprise contouritic formations. Between horizon b and the seafloor, a prograding architecture can be recognized. The thickness of the upper units increases southwards (~2 s TWTT), following the margin morphology. In the south, the sedimentary thickness decreases strongly, maximum values of ~2 s TWTT being found in the trough whereas the units are absent near the Burdwood Bank (Fig. 7b).

## Discussion

### Contourite features and bottom currents

Similar depositional and erosional features have been identified in both the Yaghan Basin and the Malvinas/Falkland depression. Nevertheless, the deepest ones occur only in the abyssal plain of the Yaghan Basin. A link between depositional/erosional features and water masses can be established, and is discussed below from shallower to greater depths.

Drift $P_a$ can be related to the AAIW (Figs. 3, 8), the terrace $T_a$ to the AAIW/UCDW interface (Fig. 3), and the drift $P_b$ to the flow of the UCDW on the upper slope of the western Yaghan Basin—evolving into an infill drift to the east of the basin (Fig. 5)—and of the Malvinas/Falkland Islands (Figs. 5, 8, 9). The $Sh_b$ drift has only been identified in the Malvinas/Falkland depression but is here also under the influence of the UCDW. In the Yaghan Basin, terrace $T_b$ and drift $M_a$ can be related to the UCDW/LCDW interface. The depth range in this area tentatively correlates with that of the SPDSW (~2,000 m; Well et al. 2003). The identified eroded surface suggests that a strongly eroding water mass flows along the northwest Scotia Sea, where it interacts with the across-slope gravity currents to cause enclosure of the middle-slope canyons. Consistent with the reported depths for the core of the LCDW in this part of the Scotia Sea (>2,000 m; Smith et al. 2010), the relatively smooth slope below this level might thus be associated with the path of the LCDW (Fig. 9).

The deeper $Sh_a$ drift reveals a net north-eastward bottom flow which must be mainly associated with SPDW (Fig. 9). $M_b$ drifts, which are associated with basement irregularities, generate the complex seafloor morphology recorded in the Yaghan Basin abyssal plain. They have in all likelihood been

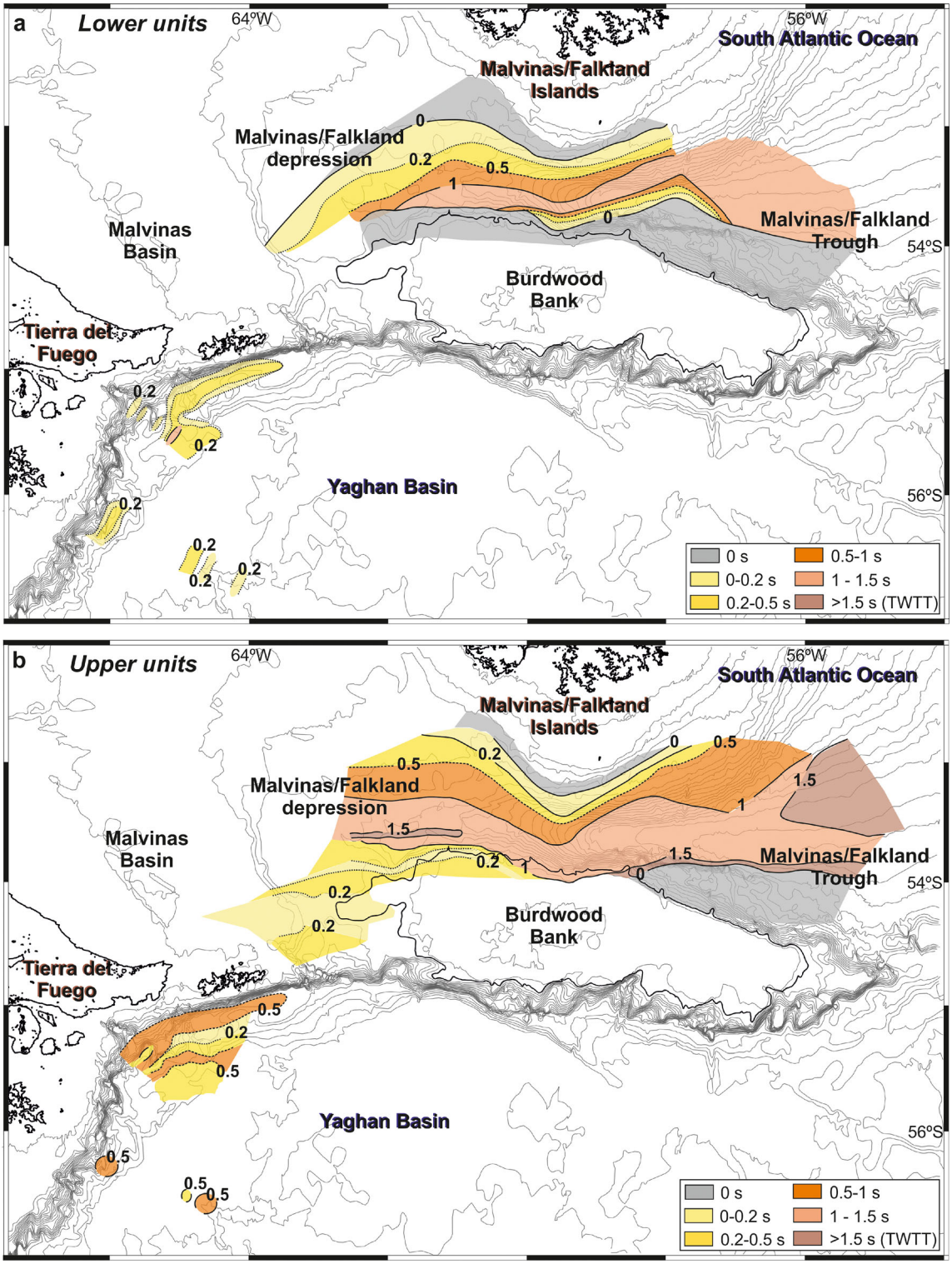


**Fig. 7** Sedimentary thickness maps (s TWTT) for **a** the lower units V and IV, and **b** the upper units III, II and I

produced by the deep-reaching eddies originating from the interaction between the SPDW and the CDW (Tarakanov 2012).

Regional geophysical and oceanographic data suggest a link between terrace $T_a$ and the depth range of the lower boundary of the AAIW (Figs. 3, 9). Since its formation, this water mass has flowed to the north, forming the upper part of the Malvinas/Falkland Current above the UCDW. The AAIW/UCDW interface and associated processes (e.g. internal waves) have contributed to the formation of other terraces in the South Atlantic—e.g. the Perito Moreno terrace (~1,000 m)

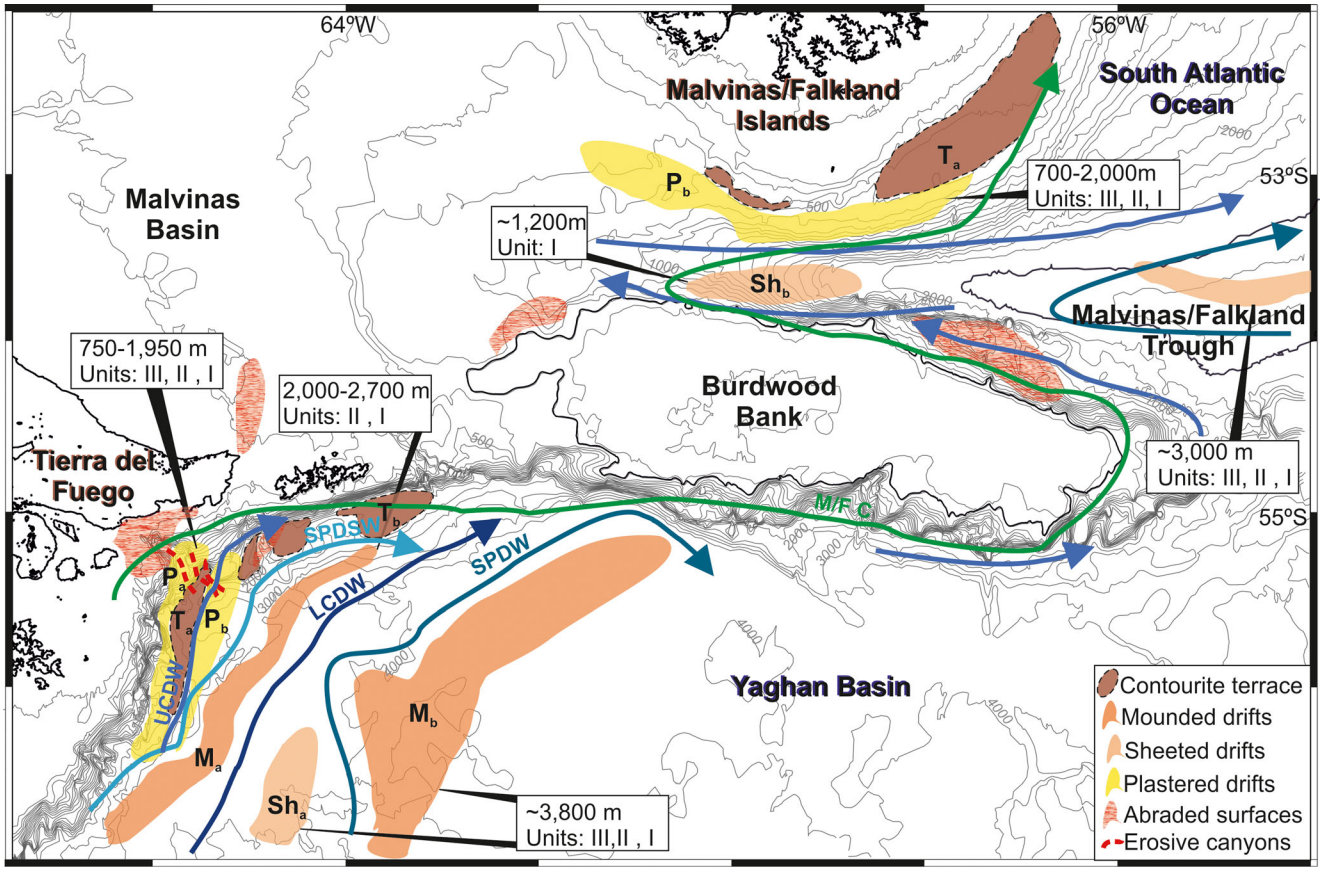


**Fig. 8** Sketch showing the locations of the main contourite drifts, contourite terraces and abraded surfaces identified in this study, together with the tentatively inferred trajectories of bottom water masses. *M/F C* Malvinas/Falkland Current. For other definitions, see Fig. 2

and the extensive Ewing terrace (~1,500 m) along the Argentinean and Uruguayan margins, both having been linked to this interface (Hernández-Molina et al. 2009; Preu et al. 2013), as well as terraces along the Brazilian margin (e.g. Borisov et al. 2013)—despite the fact that the morpho-structure along the latter margin is more complex. In contrast, based on the analysis of modern hydrographic data, Piola et al. (2013) suggested that the UCDW perhaps forms the bottom water layer over the outer part of the Perito Moreno terrace on the western slope of the Argentine Basin near 45°S. Preu et al. (2013) argued that some contourite terraces could be more actively generated by enhanced Antarctic water masses during colder periods, which is in agreement with Bozzano et al. (2011) who inferred an enhanced AAIW during glacial periods. Therefore, the role of both AAIW and UCDW in this region should be investigated for potential preservation of glacial and interglacial episodes in sediment cores. The increase in the depth range of these terraces from the northern Scotia Sea to the Uruguayan margin agrees with a slight northward deepening of the AAIW layer proposed by some authors (Matano et al. 2010; Piola et al. 2010).

Below the AAIW/UCDW interface, the identification of the $P_b$ drift in both the Yaghan Basin and the Malvinas/Falkland depression implies a north-eastward flow of the UCDW along the upper slope of the former and an eastward flow along the corresponding slope of the latter. The UCDW thus flows through the 54-54 Passage—as corroborated by the existence of abraded surfaces northeast of the Burdwood Bank—and the Shag and Black rocks passages (e.g. Arhan et al. 1999; Naveira Garabato et al. 2002a). Once in the Malvinas/Falkland depression, this water mass flows north-eastwards along the northern slope, forming the $P_b$ drift, and also westwards attached to the southern flank of the trough forming the $Sh_b$ drift.

Deeper morphologies such as those of the $T_b$, $Sh_a$, $M_a$ and $M_b$ have only been identified in the Yaghan Basin and are therefore associated with the identified water masses of the Scotia Sea. The flow of these water masses are restricted in the Malvinas/Falkland depression by the depth of the passages in the NSR. Nonetheless, the bottom current regime in the Malvinas/Falkland Trough is still being debated (Cunningham and Barker 1996; Howe et al. 1997; Cunningham et al. 1998, 2002) because the gateways along the NSR are not well constrained. The circulation patterns identified in the present study agree with a slight clockwise recirculation of the ACC west of 53°W, being forced by the eastern emplacement of the WSDW (Fig. 8). The bottom waters in the Malvinas/Falkland Trough have been attributed to north-westward overflow of

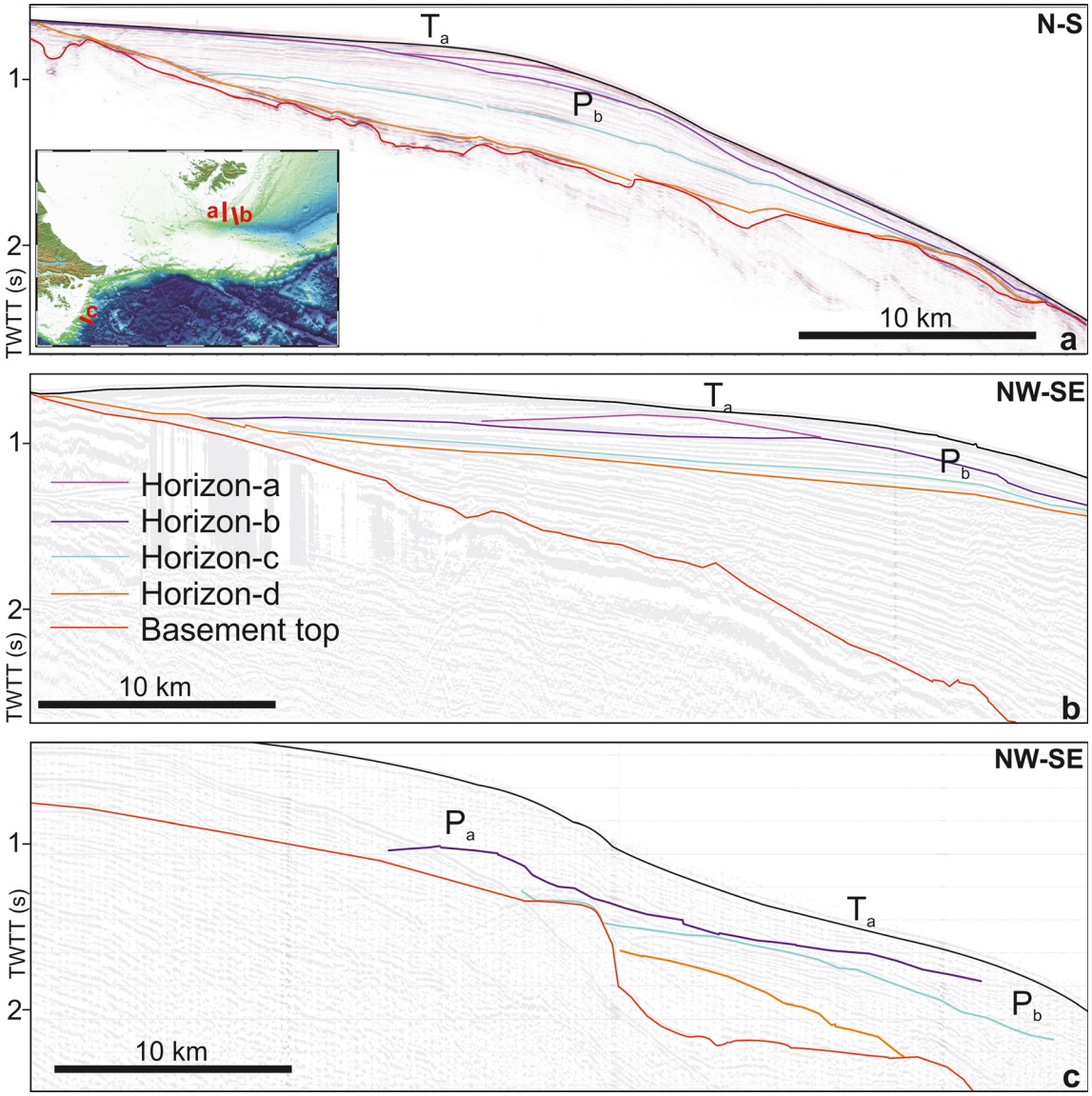


**Fig. 9** Regional overview of the contourite terrace $T_a$. **a** Interpretation of profile 1, southern slope of Malvinas/Falkland Islands (from Koenitz et al. 2008, with permission from John Wiley & Sons). **b** Line IUTIG_ rc2106-145, southern slope of Malvinas/Falkland Islands. **c** Line IT-244, western slope of Yaghan Basin

bottom waters from the Scotia Sea—namely, mixtures of WSDW and CDW (Zenk 1981). Along the NSR east of the study area, deeper gateways provide an exit for the LCDW, SPDW and WSDW (e.g. Locarnini et al. 1993; Arhan et al. 1999; Naveira Garabato et al. 2002b; Smith et al. 2010). These water masses flow eastwards, generating the eastern drifts described by previous authors (Fig. 8; Cunningham and Barker 1996; Howe et al. 1997; Cunningham et al. 1998, 2002; Koenitz et al. 2008). To the east of the trough, the northward flow has been attributed to the WSDW by Locarnini et al. (1993). Also, non-deposition on the southern margin east of 53°W is presumably related to a westward flow of WSDW (Georgi 1981; Locarnini et al. 1993). However, the lack of deposition on the northern margin can be attributed either to upward mixing of the returning WSDW into the LCDW layer or to circulation of the deepest components of the ACC (Cunningham and Barker 1996; Cunningham et al. 1998, 2002; Smith et al. 2010).

## Main tectonic features

The tectonic setting during the opening of the Drake Passage (e.g. Lawver and Gahagan 2003; Lodolo and Tassone 2010) produced the sub-vertical, south-dipping normal faults identified in the Yaghan Basin (Figs. 3a, 5a). Here, along the sub-vertical escarpment described above (between 66° and 56°W), there is an abrupt transition between the continental domain of the NSR and the oceanic domain of the Scotia Sea (Fig. 1). However, on the western side (between 68° and 66°W) the highly faulted crustal blocks denote a fringe of stretched and

tectonically overprinted continental crust resulting from the combined sheared passive margin mentioned above (Fig. 1c; Lodolo et al. 2006). The Late Cretaceous-Palaeogene compressive tectonic regime produced a series of N–NW-verging thrust faults in the NSR (Figs. 3b, 5b; Bry et al. 2004; Tassone et al. 2008). The sub-vertical normal faults identified on the northern flank of the Malvinas/Falkland depression (Figs. 3b, 4b) are related to the downward bending of the South America plate as a result of the loading generated by the Burdwood Bank and the Scotia plate (Bry et al. 2004; Koenitz et al. 2008). Consequently, and despite the ancient tectonic context, the structures observed on both flanks of the NSR were established more recently by the relative motion of the South American and Scotia plates along the present-day plate boundary (Fig. 1; Lodolo et al. 2006).

## Regional chronology

Although the amplitude and lateral continuity of the reflections are significantly reduced in the Yaghan Basin relative to those of the Malvinas/Falkland depression, the five units of the Malvinas/Falkland depression can be tentatively correlated with analogous units in the Yaghan Basin based on their stratigraphic position and the identical signature of the boundary discontinuities (Table 1). There have been several studies of the post-Jurassic stratigraphic record of the Malvinas Basin (Fig. 1b; e.g. Yrigoyen 1989; Galeazzi 1998; Tassone et al. 2008; Baristeas et al. 2013). In the present study, the five units identified in the sedimentary record of the Malvinas/Falkland depression have been included in the *upper sequence* of the Malvinas Basin, as defined by Tassone et al. (2008) and Baristeas et al. (2013), and would correspond to the fore-deep phase of the basin (42.5 Ma to Present). The overfilling stage during the development of the fore-deep is attributed to the uplifting of the fold and thrust belt during the Oligocene as a consequence of the Late Eocene compressive tectonic regime (Ghiglione et al. 2010; Baristeas et al. 2013).

Previous studies of the northern margin of the Malvinas/Falkland Trough (Koenitz et al. 2008) have correlated the main stratigraphic discontinuities in the plastered drift record with those in more remote areas such as the southern Scotia Sea (Maldonado et al. 2003) and the Agulhas Ridge (Uenzelmann-Neben 2001). The correlation between the age attribution of Koenitz et al. (2008) and the findings of the present study is shown in Table 2. The oldest unit identified in the present work (i.e. unit V) would have been formed in the Early Miocene, whereas unit IV would correspond to the Early-Middle Miocene. Both units are strongly influenced by the basement morphology (Fig. 3). Maldonado et al. (2006) assigned an age of 12.6 Ma for a widespread regional reflector identified in the southern Scotia Sea, which they called *reflector-c* and which is related to a major change in stratigraphy and depositional mode, as seen in the seismic profiles. *Reflector-c* might correspond to horizon c defined in the present work, which also marks the boundary between two different sedimentary patterns. Furthermore, the upper deposits have similar facies in both areas (e.g. wavy reflections, stratified facies and drift morphologies). According to the age correlation of Koenitz et al. (2008) and Maldonado et al. (2006), unit III would correspond to the Middle Miocene, and the two youngest units II and I to the Late Miocene-Pliocene and Late Pliocene-Quaternary respectively.

## Evolutionary model

Related to the tectonic evolution of the Drake Passage, the north-eastward elongation of the Weddell Sea subduction below the former Scotia plate during the Oligocene and the relative movement between the South America and Antarctic plates led to the establishment of a north Scotia Sea transcurrent boundary as a precursor to the present-day NSR (Eagles and Jokat 2014). The main tectonic events identified in this work are linked to the later evolution of the Drake Passage. These events, together with the ages attributed to the various sedimentary units (cf. above), can serve to establish a conceptual model comprising three main steps in the evolution of the water-mass circulation pattern.

### *Middle Miocene bottom current enhancement, AAIW onset*

The present observations tentatively suggest that the onset of $P_b$ drift sedimentation took place during the aggradational sedimentary stacking pattern of unit III, at which time the Drake Passage was already open to deep-water flows (Pagani et al. 2000). The steadier tectonic situation enabled initiation and reorganisation of the ACC through the Malvinas/Falkland Trough. It was during the Middle Miocene that the current intensity increased in the entire area, establishing the basis of the present-day circulation pattern and facilitating widespread contourite drift formation. In this context, Koenitz et al. (2008) suggested that the south Malvinas/Falkland slope drift started to develop at ca. 20.6 Ma, whereas Eagles and Jokat (2014) proposed that this drift began to be deposited with the opening of the Malvinas/Falkland Trough to frontal processes 18.5 Ma ago, during the northward propagation of the West Scotia Ridge through the NSR and into the trough. The proposed Middle Miocene age for the $P_b$ drift is consistent with a change in the bottom current regime of the Scotia Sea related to the intrusion of the WSDW through the SSR gateways (Maldonado et al. 2003), and its steadiness as the bottom water of the main abyssal plains. The enhancement of this new water mass forced the northward migration of the CDW (Pérez et al. 2014) and therefore agrees with the onset of drift formation in the northern Scotia Sea. This took place coevally with the growth of the Antarctic ice sheet (Shackleton and Kennet 1975; Zachos et al. 2001) and a general decrease in

**Table 2** Interrelations amongst discontinuities in the Malvinas/Falkland Trough (Koenitz et al. 2008), western Malvinas/Falkland Basin (Galeazzi 1998), southern Scotia Sea (Maldonado et al. 2006) and Malvinas/Falkland depression (present work), together with proposed ages

| Malvinas/Falkland Trough (Koenitz et al. 2008) | | W Malvinas/Falkland Basin (Galeazzi 1998) | | S Scotia Sea (Maldonado et al. 2006) | | This work |
|---|---|---|---|---|---|---|
| Minor unconformity within drift crest | 4.5 Ma | 1 | 5.5 Ma | Reflector-a | 3.8 Ma | ~Horizon a |
| Younger major unconformity | 9 Ma | 5 | 10.5 Ma | Reflector-b | 6.4 Ma | Horizon b |
| Minor unconformity within main drift body | 14.5 Ma | 6/7 | 12.5/13.8 Ma | Reflector-c | 12.6 Ma | Horizon c |
| Basal unconformity | 20.6 Ma | 8/11 | 15.5/21 Ma | Reflector-d | 14.9 Ma | Horizon d |

sedimentation rate around Antarctica (Handwerger and Jarrard 2003). The associated period of aggradational stacking has been recorded along the Argentinean (Hernández-Molina et al. 2010) and Uruguayan continental margins (Preu et al. 2012) and has been linked with the end of compressional tectonics in the Patagonian Cordillera (Torres Carbonell and Dimieri 2013) and a period of active subsidence (Potter and Szatmari 2009).

The $T_a$ contourite terrace has been developing offshore Tierra del Fuego since the emplacement of horizon c (Fig. 9) during the Middle Miocene—the same period as the onset of the AAIW and the AAIW/UCDW interface influence along the Argentine and Uruguayan continental slopes, generating the Perito Moreno and Ewing terraces (Hernández-Molina et al. 2009; Preu et al. 2013). Consequently, it is proposed here that the onset of the AAIW and its widespread northward circulation occurred during the Middle Miocene.

*Late Miocene SPDW inflow*

The erosional features of horizon b in the Yaghan Basin and the main drifts of its abyssal plain ($Sh_a$ and $M_b$) support the concept of enhanced CDW circulation during the Late Miocene induced by the onset of grounded ice sheets on the Antarctic Peninsula shelf (Maldonado et al. 2003). This added to the inflow of SPDW via the Drake Passage, relating to the contemporaneous shoaling of the Central American Seaway (Nisancioglu et al. 2003). The formation of energetic, deep-reaching eddies (Tarakanov 2012) through the interaction of the SPDW with the LCDW probably generated the irregular seafloor morphology and the formation of drifts attached to the acoustic basement highs (Fig. 5b).

Due to the regional deepening, the $P_b$ drift of the Malvinas/Falkand slope progradated from horizon b in response to the compression generated by the transpressive regime along the northern margin of the Burdwood Bank after the cessation of the West Scotia Ridge activity (Richards et al. 1996; Maldonado et al. 2000; Bry et al. 2004), which produced a change in the sedimentary pattern along the northern flank of the NSR. The Argentinean margin responded in similar manner, as evidenced by the onset of oceanward progradation of sedimentary sequences and a halt in the growth of giant drifts during the Late Miocene-Early Pliocene (Hernández-Molina et al. 2009, 2010; Preu et al. 2013).

*Late Pliocene bottom current enhancement*

The growing drifts in unit I and the formation of certain widespread drifts, which include the $Sh_b$ and the plastered drift identified in the Malvinas Basin by Baristeas et al. (2013), reveal an enhancement of bottom currents during the Late Pliocene. This was coeval with the final closure of the Central America Seaway and the onset of glaciations in the

Northern Hemisphere (e.g. Nisancioglu et al. 2003; Bartoli et al. 2005). This, in turn, was coeval with the final cessation of Phoenix Ridge activity (Maldonado et al. 2000) and with the expansion of Antarctic ice sheets (McKay et al. 2012).

## Conclusions

This study has demonstrated that the identification of contourite features on the present-day seafloor and within the sedimentary record provides the key for the decoding of past water-mass circulation and the identification of major palaeoceanographic events. At the transition between the western Scotia Sea and southern South Atlantic Ocean, each major drift is developed in a water depth range coincident with a particular water mass, the contourite terraces on top of certain drifts being associated with the interfaces between water masses.

Two major palaeoceanographic changes have been identified: (1) the onset of Antarctic Intermediate Water flow and the enhancement of Circumpolar Deep Water flow in the Middle Miocene, which were coeval with the onset of Weddell Sea Deep Water flow in the Scotia Sea. This conditioned the onset of the development of present-day large contourite features along the slope. (2) The onset of Southeast Pacific Deep Water flow and its complex interaction with Lower Circumpolar Deep Water in the abyssal plain of the Yaghan Basin in the Late Miocene. The resulting new oceanographic scenario mainly initiated the present-day deepest seafloor morphologies. Interestingly, the two periods of changing bottom currents were coincident with regional tectonic episodes, as well as with climate and Antarctic ice sheet oscillations. Therefore, a very attractive line of research would be the linking of internal and external processes and, in particular, the establishment of a more robust chronology through scientific drilling.

**Acknowledgements** L.F.P. acknowledges a JAE predoctoral studentship from CSIC, and the IAS Postgraduate Grant Scheme for providing travel support. We thank colleagues from the University of Buenos Aires for assistance, and colleagues from the Istituto Nazionale di Oceanografia e di Geofisica Sperimentale (OGS) of Trieste for seismic processing of TM data. This work forms part of ongoing projects CTM2008-06386-C02/ANT and CTM2011-30241-C02, with links to projects CTM2012-39599-C03, IGCP-619 and INQUA 1204. It was part-funded by the COMPASS consortium, and done in collaboration with the Continental Margins Research Group of the Royal Holloway University of London. We acknowledge John Wiley & Sons for permission to reuse Figure 4a from Koenitz et al. (2008). We thank two anonymous reviewers and the editors for constructive comments which helped improve the paper.

**Conflict of interest** The authors declare that they have no conflict of interest.

## References

Anderson LM, Davison I, Gormly P, Nuttall P (2010) Hydrocarbon prospectivity of the North Scotian Fold Belt and the South Malvinas Basin. In: Proc 72nd European Association of Geoscientists and Engineers Conf Exhib, Society of Petroleum Engineers & EUROPEC, Barcelona, pp 5100–5104

Arhan M, Heywood KJ, King BA (1999) The deep waters from the Southern Ocean at the entry to the Argentine Basin. Deep-Sea Res II 46:475–499

Baristeas N, Anka Z, di Primio R, Rodriguez JF, Marchal D, Dominguez F (2013) New insights into the tectono-stratigraphic evolution of the Malvinas Basin, offshore of the southernmost Argentinean continental margin. Tectonophysics 604:280–295. doi:10.1016/j.tecto.2013.06.009

Barker PF, Thomas E (2004) Origin, signature and palaeoclimatic influence of the Antarctic Circumpolar Current. Earth Sci Rev 66:143–162

Bartoli G, Sarnthein M, Weinelt M, Erlenkeuser H, Garbe-Schönberg D, Lea DW (2005) Final closure of Panama and the onset of northern hemisphere glaciation. Earth Planet Sci Lett 237:33–44. doi:10.1016/j.epsl.2005.06.020

Borisov DG, Murdmaa IO, Ivanova EV, Levchenko OV, Yutsis VV, Frantseva TN (2013) Contourite systems in the region of the southern São Paulo Plateau escarpment. South Atlantic Oceanol 53:460–471. doi:10.1134/s0001437013040012

Bozzano G, Violante RA, Cerredo ME (2011) Middle slope contourite deposits and associated sedimentary facies off NE Argentina. Geo-Mar Lett 31:495–507. doi:10.1007/s00367-011-0239-x

Bry M, White N, Singh S, England R, Trowell C (2004) Anatomy and formation of oblique continental collision: South Falkland basin. Tectonics 23:4011–4020. doi:10.1029/2002TC001482

Cunningham WD (1993) Strike-slip faults in the southernmost Andes and the development of the Patagonian orocline. Tectonics 12:169–186

Cunningham AP, Barker PF (1996) Evidence for westward-flowing Weddell Sea Deep Water in the Falkland Trough, western South Atlantic. Deep-Sea Res I 43:643–654

Cunningham AP, Barker PF, Tomlinson JS (1998) Tectonics and sedimentary environment of the North Scotia Ridge region revealed by side-scan sonar. J Geol Soc 155:941–956

Cunningham AP, Howe JA, Barker PF (2002) Contourite sedimentation in the Falkland Trough, western South Atlantic. Geol Soc Memo 22:337–352. doi:10.1144/GSL.MEM.2002.022.01.24

Davey FJ (1972) Gravity measurements over Burdwood. Bank. Mar Geophys Res 1:428–435

Deacon GER (1933) A general account of the hydrology of the South Atlantic Ocean. Discovery Reports 7:171–238

Eagles G, Jokat W (2014) Tectonic reconstructions for paleobathymetry in Drake Passage. Tectonophysics 611:28–50. doi:10.1016/j.tecto.2013.11.021

Ewing JI, Ludwig WJ, Ewing M, Eittreim SL (1971) Structure of the Scotia Sea and Falkland Plateau. J Geophys Res 76(29):7118–7137

Faugères JC, Stow DAV (2008) Contourite drifts. Nature, evolution and controls. In: Rebesco M, Camerlenghi A (eds) Developments in sedimentology, vol 60. Elsevier, Amsterdam, pp 259–288

Faugères JC, Stow DAV, Imbert P, Viana A (1999) Seismic features diagnostic of contourite drifts. Mar Geol 162:1–38

Galeazzi JS (1998) Structural and stratigraphic evolution of the western Malvinas Basin, Argentina. AAPG Bull 82:596–636

Galindo-Zaldivar J, Bohoyo F, Maldonado A, Schreider A, Suriñach E, Vázquez JT (2006) Propagating rift during the opening of a small oceanic basin: the Protector Basin (Scotia Arc, Antarctica). Earth Planet Sci Lett 241:398–412

Geletti R, Lodolo E, Schreider AA, Polonia A (2005) Seismic structure and tectonics of the Shackleton Fracture Zone (Drake Passage, Scotia Sea). Mar Geophys Res 26:17–28

Georgi DT (1981) Circulation of bottom waters in the southwestern Atlantic. Deep-Sea Res 28:959–979

Ghiglione MC, Quinteros J, Yagupsky D, Bonillo-Martínez P, Hlebszevtich J, Ramos VA, Vergani G, Figueroa D, Quesada S, Zapata T (2010) Structure and tectonic history of the foreland basins of southernmost South America. J S Am Earth Sci 29:262–277. doi:10.1016/j.jsames.2009.07.006

Handwerger DA, Jarrard RD (2003) Neogene changes in Southern Ocean sedimentation based on mass accumulation rates at four continental margins. Paleoceanography 18:1081. doi:10.1029/2002PA000850

Hernández-Molina FJ, Paterlini M, Violante R, Marshall P, de Isasi M, Somoza L, Rebesco M (2009) Contourite depositional system on the Argentine Slope: an exceptional record of the influence of Antarctic water masses. Geology 37:507–510

Hernández-Molina FJ, Paterlini M, Somoza L, Violante R, Arecco MA, de Isasi M, Rebesco M, Uenzelmann-Neben G, Neben S, Marshall P (2010) Giant mounded drifts in the Argentine Continental Margin: origins, and global implications for the history of thermohaline circulation. Mar Petrol Geol 27:1508–1530. doi:10.1016/j.marpetgeo.2010.04.003

Hernández-Molina FJ, Llave E, Preu B, Ercilla G, Fontan A, Bruno M, Serra N, Gomiz JJ, Brackenridge RE, Sierro FJ, Stow DAV, Garcia M, Juan C, Sandoval N, Arnaiz A (2014) Contourite processes associated with the Mediterranean Outflow Water after its exit from the Strait of Gibraltar: global and conceptual implications. Geology 42:227–230. doi:10.1130/G35083.1

Howe JA, Pudsey CJ, Cunningham AP (1997) Pliocene-Holocene contourite deposition under the Antarctic Circumpolar Current, western Falkland Trough, South Atlantic Ocean. Mar Geol 138:27–50

Ingle JC Jr (2000) Deep-sea and global ocean circulation. In: Ernst WG (ed) Earth systems: processes and issues. Cambridge University Press, Cambridge, pp 169–181

Kennett JP (1977) Cenozoic evolution of Antarctic glaciation, the Circum-Antarctic ocean, and their impact on global paleoceanography. J Geophys Res 82:3843–3860

Klepeis KA, Austin JA (1997) Contrasting styles of superposed deformation in the southernmost Andes. Tectonics 16:755–776. doi:10.1029/97TC01611

Koenitz D, White N, McCave IN, Hobbs R (2008) Internal structure of a contourite drift generated by the Antarctic Circumpolar Current. Geochem Geophys Geosyst 9, Q06012. doi:10.1029/2007GC001799

Lawver LA, Gahagan LM (2003) Evolution of Cenozoic seaways in the circum-Antarctic region. Palaeogeogr Palaeoclimatol Palaeoecol 198:11–37

Locarnini RA, Whitworth T III, Nowlin WD Jr (1993) The importance of the Scotia Sea on the outflow of Weddell Sea Deep Water. J Mar Res 51:135–153

Lodolo E, Tassone A (2010) Gateways and climate: the Drake Passage opening. Boll Geofis Teor Appl 51:77–88

Lodolo E, Menichetti M, Bartole R, Ben-Avraham Z, Tassone A, Lippai H (2003) Magallanes-Fagnano continental transform fault (Tierra del Fuego, southernmost South America). Tectonics 22:15-11–15-26. doi:10.1029/2003TC001500

Lodolo E, Donda F, Tassone A (2006) Western Scotia Sea margins: improved constraints on the opening of the Drake Passage. J Geophys Res B 111, B06101. doi:10.1029/2006JB004361

Ludwig WJ, Rabinowitz PD (1982) The collision complex of the North Scotia Ridge. J Geophys Res 87:3731–3740

Ludwig WJ, Ewing JI, Ewing M (1968) Structure of Argentine Continental Margin. Am Assoc Petrol Geol B 52:2337–2368

Maldonado A, Balanyá JC, Barnolas A, Galindo-Zaldivar J, Hernández J, Jabaloy A, Livermore R, Martínez-Martínez JM, Rodríguez-Fernández J, De Galdeano CS, Somoza L, Surinach E, Viseras C (2000) Tectonics of an extinct ridge-transform intersection, Drake Passage (Antarctica). Mar Geophys Res 21:43–67

Maldonado A, Barnolas A, Bohoyo F, Galindo-Zaldivar J, Hernández-Molina J, Lobo F, Rodríguez-Fernández J, Somoza L, Vázquez JT (2003) Contourite deposits in the central Scotia Sea: the importance of the Antarctic Circumpolar Current and the Weddell Gyre flows. Palaeogeogr Palaeoclimatol Palaeoecol 198:187–221. doi:10.1016/S0031-0182(03)00401-2

Maldonado A, Bohoyo F, Galindo-Zaldívar J, Hernández-Molina FJ, Jabaloy A, Lobo FJ, Rodríguez-Fernández J, Suriñach E, Vázquez JT (2006) Ocean basins near the Scotia - Antarctic plate boundary: influence of tectonics and paleoceanography on the Cenozoic deposits. Mar Geophys Res 27(2):83–107. doi:10.1007/s11001-006-9003-4

Maldonado A, Bohoyo F, Galindo-Zaldívar J, Hernández-Molina FJ, Lobo FJ, Lodolo E, Martos YM, Pérez LF, Schreider AA, Somoza L (2014) A model of oceanic development by ridge jumping: opening of the Scotia Sea. Global Planet Change 123:152–173. doi:10.1016/j.gloplacha.2014.06.010

Matano RP, Palma ED, Piola AR (2010) The influence of the Brazil and Malvinas Currents on the Southwestern Atlantic Shelf circulation. Ocean Sci 6:983–995. doi:10.5194/os-6-983-2010

McKay R, Naish T, Carter L, Riesselman C, Dunbar R, Sjunneskog C, Winter D, Sangiorgi F, Warren C, Pagani M, Schouten S, Willmott V, Levy R, DeConto R, Powell RD (2012) Antarctic and Southern Ocean influences on Late Pliocene global cooling. Proc Natl Acad Sci U S A 109:6423–6428. doi:10.1073/pnas.1112248109

Meredith MP, Garabato ACN, Stevens DP, Heywood KJ, Sanders RJ (2001) Deep and bottom waters in the Eastern Scotia sea: rapid changes in properties and circulation. J Phys Oceanogr 31:2157–2168. doi:10.1175/1520-0485(2001)031<2157:DABWIT>2.0.CO;2

Morozov EG, Demidov AN, Tarakanov RY, Zenk W (2010) Abyssal channels in the Atlantic Ocean. Springer, Berlin

Muñoz A, Cristobo J, Rios P, Druet M, Polonio V, Uchupi E, Acosta J (2012) Sediment drifts and cold-water coral reefs in the Patagonian upper and middle continental slope. Mar Petrol Geol 36:70–82. doi:10.1016/j.marpetgeo.2012.05.008

Naveira Garabato AC, Heywood KJ, Stevens DP (2002a) Modification and pathways of Southern Ocean Deep Waters in the Scotia Sea. Deep-Sea Res I 49:681–705

Naveira Garabato AC, McDonagh EL, Stevens DP, Heywood KJ, Sanders RJ (2002b) On the export of Antarctic Bottom Water from the Weddell Sea. Deep-Sea Res II 49:4715–4742

Naveira Garabato AC, Stevens DP, Heywood KJ (2003) Water mass conversion, fluxes, and mixing in the Scotia Sea diagnosed by an inverse model. J Phys Oceanogr 33:2565–2587

Nisancioglu KH, Raymo ME, Stone PH (2003) Reorganisation of Miocene deep water circulation in response to the shoaling of the Central American Seaway. Paleoceanography 18:1006–1018. doi:10.1029/2002PA000767

Orsi AH, Johnson GC, Bullister JL (1999) Circulation, mixing, and production of Antarctic Bottom Water. Prog Oceanogr 43:55–109

Owen MJ, Day SJ, Leat PT, Tate AJ, Martin TJ (2014) Control of sedimentation by active tectonics, glaciation and contourite-depositing currents in Endurance Basin, South Georgia. Global Planet Change 123:323–343. doi:10.1016/j.gloplacha.2014.08.003

Pagani M, Arthur MA, Freeman KH (2000) Variations in Miocene phytoplankton growth rates in the southwest Atlantic: evidence for changes in ocean circulation. Paleoceanography 15:486–496. doi:10.1029/1999PA000484

Pérez LF, Lodolo E, Maldonado A, Hernández-Molina FJ, Bohoyo F, Galindo-Zaldívar J, Lobo FJ (2014) Tectonic development,

sedimentation and paleoceanography of the Scan Basin (Southern Scotia Sea, Antarctica). Global Planet Change 123:344–358. doi:10.1016/j.gloplacha.2014.06.007

Peterson RG, Whitworth T III (1989) The subantarctic and polar fronts in relation to deep water masses through the Southwestern Atlantic. J Geophys Res 94(C8):10817–10838

Piola AR, Gordon AL (1989) Intermediate waters in the southwest South Atlantic. Deep-Sea Res I 36:1–16

Piola AR, Martínez Avellaneda N, Guerrero RA, Jardón FP, Palma ED, Romero SI (2010) Malvinas-slope water intrusions on the northern Patagonia continental shelf. Ocean Sci 6:345–359. doi:10.5194/os-6-345-2010

Piola AR, Franco BC, Palma ED, Saraceno M (2013) Multiple jets in the Malvinas Current. J Geophys Res Oceans 118:2107–2117. doi:10.1002/jgrc.20170

Platt NH, Philip PR (1995) Structure of the southern Falkland Islands continental shelf: initial results from new seismic data. Mar Petrol Geol 12:759–771

Potter PE, Szatmari P (2009) Global Miocene tectonics and the modern world. Earth Sci Rev 96:279–295

Preu B, Schwenk T, Hernández-Molina FJ, Violante R, Paterlini M, Krastel S, Tomasini J, Spieß V (2012) Sedimentary growth pattern on the northern Argentine slope: the impact of North Atlantic Deep Water on southern hemisphere slope architecture. Mar Geol 329–331:113–125. doi:10.1016/j.margeo.2012.09.009

Preu B, Hernández-Molina FJ, Violante R, Piola AR, Paterlini CM, Schwenk T, Voigt I, Krastel S, Spiess V (2013) Morphosedimentary and hydrographic features of the northern Argentine margin: the interplay between erosive, depositional and gravitational processes and its conceptual implications. Deep-Sea Res I 75:157–174. doi:10.1016/j.dsr.2012.12.013

Provost C, Renault A, Barré N, Sennéchael N, Garçon V, Sudre J, Huhn O (2011) Two repeat crossings of Drake Passage in austral summer 2006: short-term variations and evidence for considerable ventilation of intermediate and deep waters. Deep-Sea Res II 58:2555–2571. doi:10.1016/j.dsr2.2011.06.009

Rebesco M (2005) Contourites. In: Richard C, Selley RC, Cocks LRM, Plimer IR (eds) Encyclopedia of geology, vol 4. Elsevier, London, pp 513–527

Rebesco M, Hernández-Molina FJ, Van Rooij D, Wåhlin A (2014) Contourites and associated sediments controlled by deep-water circulation processes: state-of-the-art and future considerations. Mar Geol 352:111–154

Richards PC, Gatliff RW, Quinn MF, Fannin NGT, Williamson JP (1996) The geological evolution of the Falkland Islands continental shelf. Geol Soc Lond Spec Publ 108:105–128. doi:10.1144/gsl.sp.1996.108.01.08

Sandwell DT, Smith WHF (1997) Marine gravity anomaly from Geosat and ERS 1 satellite altimetry. J Geophys Res B 102:10039–10054

Schlitzer R (2013) Ocean Data View. http://odv.awi.de

Shackleton NJ, Kennet JP (1975) Paleotemperature history of the Cenozoic and the initiation of Antarctic Glaciation: oxygen and carbon isotope analyses in DSDP sites 272, 279, and 281. Deep Sea Drilling Project Rep Publ 29:743–755

Sievers HA, Nowlin WD (1984) The stratification and water masses at Drake Passage. J Geophys Res Oceans 89:10489–10514. doi:10.1029/JC089iC06p10489

Smith IJ, Stevens DP, Heywood KJ, Meredith MP (2010) The flow of the Antarctic Circumpolar Current over the North Scotia Ridge. Deep-Sea Res I 57:14–28

Stow DAV, Pudsey CJ, Howe JA, Faugères J-C, Viana AR (eds) (2002) Deep-water contourite systems: modern drifts and ancient series. Seismic and sedimentary characteristics. Geological Society, London, Memoir no 22

Tarakanov RY (2009) Antarctic bottom water in the Scotia Sea and the Drake Passage. Oceanology 49:607–621

Tarakanov RY (2012) The Scotia Sea and the Drake Passage as an orographic barrier for the Antarctic Circumpolar Current. Oceanology 52:157–170

Tassone A, Lodolo E, Menichetti M, Yagupsky D, Caffau M, Vilas JF (2008) Seismostratigraphic and structural setting of the Malvinas Basin and its southern margin (Tierra del Fuego Atlantic offshore). Geol Acta 6(1):55–67

Torres Carbonell PJ, Dimieri LV (2013) Cenozoic contractional tectonics in the Fuegian Andes, southernmost South America: a model for the transference of orogenic shortening to the foreland. Geol Acta 11:331–357. doi:10.1344/105.000001874

Uenzelmann-Neben G (2001) Seismic characteristics of sediment drifts: an example from the Agulhas Plateau, southwest Indian Ocean. Mar Geophys Res 22:323–343

Viana AR (2001) Seismic expression of shallow- to deep-water contourites along the south-eastern Brazilian margin. Mar Geophys Res 22:509–521

Well R, Roether W, Stevens DP (2003) An additional deep-water mass in Drake Passage as revealed by $^{3}$He data. Deep-Sea Res I 50:1079–1098. doi:10.1016/S0967-0637(03)00050-5

Wittstock RR, Zenk W (1983) Some current observations and surface T/S distribution from the Scotia Sea and the Bransfield Strait during early austral summer 1980/1981. Meteor Forschungs-Ergebnisse Reihe A/B 24:77–86

Yrigoyen MR (1989) Cuenca de Malvinas. In: Chebli GA, Spalletti LA (eds) Cuencas sedimentarias Argentinas: Correlación Geológica, vol 6. Universidad Nacional del Tucumán, pp 481–491

Zachos J, Pagani H, Sloan L, Thomas E, Billups K (2001) Trends, rhythms, and aberrations in global climate 65 Ma to present. Science 292:686–693

Zenk W (1981) Detection of overflow events in the Shag Rocks Passage, Scotia Ridge. Science 213:1113–1114. doi:10.1126/science.213.4512.1113